Cancer Letters 336 (2013) 174–184

Contents lists available at SciVerse ScienceDirect

Cancer Letters

journal homepage: www.elsevier.com/locate/canlet

IFN-γ selectively exerts pro-apoptotic effects on tumor-initiating label-retaining colon cancer cells

Chao Ni [a,1], Ping Wu [a,1], Xiaotao Zhu [b], Jun Ye [a], Zhigang Zhang [a], Zhigang Chen [a], Ting Zhang [c], Tao Zhang [a], Ke Wang [a], Dang Wu [a], Fuming Qiu [c], Jian Huang [a,c,*]

[a] Cancer Institute (Key Laboratory of Cancer Prevention & Intervention, National Ministry of Education, Provincial Key Laboratory of Molecular Biology in Medical Sciences), The Second Affiliated Hospital, Zhejiang University School of Medicine, Hangzhou 310009, China
[b] Jinhua Central Hospital, Jinhua 321000, China
[c] Department of Oncology, Second Affiliated Hospital, Zhejiang University School of Medicine, Hangzhou 310009, China

ARTICLE INFO

Article history:
Received 25 January 2013
Received in revised form 1 April 2013
Accepted 26 April 2013

Keywords:
Cancer stem cells
Quiescent cancer cells
Lgr5
Interferon gamma
Apoptosis

ABSTRACT

Label-retaining cancer cells (LRCCs) represent a novel population of stem-like cancer cells exhibiting slow cycling, chemoresistance and tumor-initiating capacities; however, their properties remain unclear, and approaches to eradicate LRCCs remain elusive. Here, we report that colon cancer cells with high fluorescent intensity, referred to as LRCCs, have the greatest cancer stem cell (CSC)-like capacities and that they preferentially express CSC markers and stemness-related genes. Moreover, we found that Lgr5, which has been reported to be a marker of rapid cycling CSCs, is almost negatively expressed in LRCCs but that its expression is gradually increased in the differentiation process of LRCCs. Interestingly, we found that LRCCs are especially sensitive to the pro-apoptotic effect of IFN-γ treatment both *in vitro* and *in vivo* because LRCCs possess higher IFN-γR levels compared with non-LRCCs, which results in the upregulation of the apoptosis pathway after IFN-γ treatment. Furthermore, we found that IFN-γ shows synergistic effects with the conventional anticancer drug Oxaliplatin to eliminate both LRCCs and non-LRCCs. In conclusion, this is the first study to suggest that LRCCs, as a distinct tumor-initiating population, can be selectively eradicated by IFN-γ, which may provide a novel therapeutic strategy for colon cancer treatment.

1. Introduction

Cancer stem cells (CSCs) represent a relatively rare population of cells that proliferate slowly, are highly resistant to drugs, and possess tumor-initiating capacities. Currently, the most common method of defining CSCs is based on various cell surface markers, which have been demonstrated to enrich stem-like cancer cells. However, there is still some controversy surrounding these surface markers. CD133+ and CD44+/CD24+ have been used as typical exemplified CSC markers in colon cancer [1,2], but several researchers have found that both CD133+ and CD133− colon cancer cells display similar capacities in colon sphere formation and serial xenograft formation; CD133− tumor cells show more aggressive behavior during metastasis [3]. Furthermore, the great variation of CD44 and CD24 expression in patients raises questions about their usefulness as CSC markers [4]. Because the majority of markers currently used to identify CSCs are non-specific and their functions have not been clarified [5–7], we focused our study on distinct subpopulations of cancer cells with specific characteristics, such as quiescence or slow proliferation that are arrested in the G0 phase of the cell cycle. Although PY-Hoechst 33342 double staining can directly isolate cells in the G0 phase, the cytotoxicity of dyes limits live sorting [8]. Because the label retention assay is now considered an effective approach to isolate quiescent cancer cells in a solid tumor [9], in this study, we used PKH26/67 staining of primary colon cancer cells. We sorted the cells by fluorescence intensity into PKH^{hi}, PKH^{low} and PKH^{neg} subsets, but only the PKH^{hi} subset of cells is referred to as LRCCs.

Mirroring normal adult stem cells, quiescence and slow proliferation are important features of CSCs, and recent reports have further confirmed the critical function of quiescent cancer cells in tumor initiation [10]. However, increasing evidence has indicated that there is another subpopulation of intestinal stem cells or colon CSCs that exhibit rapid cycling properties, which are marked with Lgr5 positive expression [11,12]. In this study, first, we demonstrated that PKH^{hi} cells strongly exhibit stem-like properties, including tumor initiating capacity, colony formation, and chemoresistance, as well as the expression of CSC markers and stemness-related genes. Next, we found that LRCCs express Lgr5 at low levels but that its expression is gradually increased during LRCC proliferation, which strongly im-

* Corresponding author. Address: Department of Oncology, Second Affiliated Hospital, Zhejiang University School of Medicine, Hangzhou 310009, China. Tel.: +86 571 87315009; fax: +86 571 87022776.
E-mail address: drhuangjian@zju.edu.cn (J. Huang).
[1] These authors are contributed equally to this work.

0304-3835/$ - see front matter © 2013 Elsevier Ireland Ltd. All rights reserved.
http://dx.doi.org/10.1016/j.canlet.2013.04.029

plies that Lgr5+ cells could be derived from LRCCs. However, a specific approach to eradicate LRCCs is still unknown.

CSCs escape immune surveillance through the low expression of MHC molecules, resulting in the inhibition of anti-tumor immune cell activation and the inhibition of regulatory T (Treg) cell induction [13,14]. Meanwhile, specific anti-cancer cytokines can potentially eliminate CSC-like cells. Type I interferons, IFN-α and IFN-β, have been reported to target CSC-like cells in both ovarian cancer and glioblastoma [15,16], which implies that these cytokines may be useful for restoring anti-cancer functions.

IFN-γ is the only member of the Type III FN family and has long been clinically used for anti-cancer treatment [17–22]. Its anti-cancer functions include tumor surveillance by the immune system, anti-angiogenic functions, cell cycle restriction and pro-apoptotic functions [23]. It has been shown that cell cycle suppression could greatly potentiate the pro-apoptotic function of IFN-γ [24–26], which piqued our interest and prompted us to study its effect on quiescent subset-PKH^{hi} cells. Here, we first report that the quiescent cancer cells with stem cell-like properties are especially sensitive to the apoptotic effect of IFN-γ, due to their overexpression of IFN-γ receptors. Furthermore, we report that IFN-γ synergistically combined with Oxaliplatin (Oxa), a first-line colon cancer chemotherapy drug, can eradicate both LRCCs and non-LRCCs, which significantly inhibits tumor growth and reduces the risk of serial tumor formation.

To the best of our knowledge, we report for the first time that LRCCs, as a distinct subpopulation of CSCs, can be selectively eliminated by IFN-γ treatment, which may provide a novel therapeutic strategy for colon cancer treatment.

2. Materials and methods

2.1. Primary colon cancer cell preparation and cell lines

The P1, P2 and P3 cells were primary cancer cells isolated from human colon adenocarcinoma specimens obtained during surgical procedures, which was approved by the Research Ethics Board at Zhejiang University. Informed consent was obtained from each patient. The preparation of primary tumor cells P2 and P3 was performed as we have described previously with some modifications [28]. Briefly, tumor bulks were washed in phosphate-buffered saline and minced completely with sterile scalpel blades, followed by incubation with serum-free (SF) DMEM F12 (Invitrogen, Grand Island, NY) medium supplemented with 1 mg/ml Collagenase Type IV and 1 mg/ml hyaluronidase (Worthington, Lakewood, NJ) for 1.5 h at 37 °C to obtain a single cell suspension. Erythrocytes and tissue debris were removed from the cell suspension with density gradient centrifugation on ficoll (1.077 g/ml) at 400 g for 15 min. The cell pellet was resuspended in DMEM F12 medium containing 10% FBS (Invitrogen, Carlsbad, CA) with a density of ~10 cells/ml. Then, a 100 μl single cell suspension was seeded into each well of a 96-well plate, and the wells containing only a single cell were marked. In the following days, these marked wells were checked with a phase-contrast microscope to exclude wells with fibroblast growth. The tumor cell colonies were transferred to six-well plates when the cells reached confluency; then, the cells were divided, with one portion used for subsequent experiments and one portion frozen.

P1 cancer cells were established earlier in our lab from a liver metastatic lesion from a patient diagnosed with a colon adenocarcinoma [28]. P1 cancer cells were cultured in RPMI-1640 (Invitrogen, Grand Island, NY) medium containing 10% FBS. Colon cancer cell line HT29 was maintained in McCoy's 5A (Invitrogen, Grand Island, NY) medium containing 10% FBS. The HT29 and HCT116 cell lines were obtained from the American Type Culture Collection.

2.2. Cell staining and isolation

The cells were stained with PKH26/67, which irreversibly binds to the lipid bilayer of cell membranes; moreover, the expression of PKH26/67 is divided equally among the daughter cells subsequent to each cell cycle. Cancer cells were then sorted on the basis of their different fluorescent intensities, which were then classified as the PKH^{hi}, PKH^{low} and PKH^{neg} subsets (gated at >10^3 fluorescence units, 10^2–10^3 fluorescence units and <10^2 fluorescence units, respectively) both *in vitro* and *in vivo* (Supplementary data: materials and methods).

2.3. Sphere formation and FACS procedures

Cells were suspended in Diluents C (~1×10^7 cells/ml) and then labeled with PKH26/PKH67 (2×10^{-6} M, 5 min). The staining efficiency was greater than 99%. A total of 1000 cells/well were cultured in SF-DMEM, containing F-12 (Invitrogen, Grand Island, NY) medium supplemented with 10 ng/ml epidermal growth factor, 10 ng/ml basic fibroblast growth factor, N2 (Invitrogen, Grand Island, NY) and 4 μg/ml heparin (Sigma–Aldrich, St. Louis, MO), on ultralow attachment six-well plates (Corning Life Sciences, Acton, MA). The spheroids were cultured for 2 weeks. The ratio of spheroid formation was calculated according to the primary seeded cell number.

PKH^{hi}, PKH^{low} and PKH^{neg} cells were obtained both *in vitro* and *in vivo*. Single cells were selected from the spheroids with Accutase (Invitrogen, Grand Island, NY, 37 °C, 5 min, and filtered through a 40 μm strainer) and dissociated *in vitro*. While *in vivo*, tumor cells (2×10^6) were stained with PKH26 and suspended in 100 μl of medium composed of 1:1 DMEM F-12 and Matrigel (BD pharmingen, San Diego, CA, USA). Cells were injected s.c into 4- to 5-week-old male nude mice. After 14 days, single cell suspensions were obtained from xenograft tumors using the same method utilized for primary tumor bulks. Cells either *in vitro* or *in vivo* were subjected to FACS analysis with a BD Aria II flow cytometer (BD Biosciences, San Jose, CA) to yield PKH^{hi}, PKH^{low} and PKH^{neg} cells.

2.4. Soft agar colony formation assay

A soft agar colony formation assay was performed to compare the colony formation ability of PKH^{hi}, PKH^{low} and PKH^{neg} cells. The assays were previously described [28].

2.5. Flow cytometry analysis

To investigate the cell cycle changes after IFN-γ (human recombinant IFN-γ, rhIFN-γ, R&D systems, USA) treatment, cells were harvested and fixed by 95% ethanol (4 °C, overnight) and then incubated with RNase A (50 μg/ml, 30 min; Roche Applied Science, Indianapolis, IN) and stained with PI (50 μg/ml, 30 min). The intracellular PI fluorescence intensity was measured by flow cytometry (FCM), and sub-G0/1 phase was considered to be apoptosis. To verify the quiescent trait of label-retaining cells (LRCs), single cell suspensions from spheroids were incubated with cell culture medium containing 10 μg/ml Hoechst 33342 (37 °C, 45 min), and 5 μg/ml PY was added for a further 15 min incubation using the same conditions. The cells with low PY staining were identified at G0 phase.

To detect the CSC markers and IFN-γR distribution, xenografts were dissociated into single cells and washed twice with PBS. The CD133 (APC-conjugated, Miltenyi biotec, Bergisch Gladbach, Germany), CD24 (APC-conjugated, Miltenyi biotec, Bergisch Gladbach, Germany), CD44 (FITC-conjugated, Miltenyi biotec, Bergisch Gladbach, Germany), ki67 (Alexafluor 647-conjugated, Biolegend, San Diego, CA) and IFNGR-β (PE-conjugated, Biolegend, San Diego, CA) antibodies were used for direct staining. An indirect labeling method was used to stain LGR5 (Abgent, San Diego, CA) and IFNGR-α (Biolegend, San Diego, CA), and the secondary antibodies used were Dylight 488/647-conjugated (Biolegend, San Diego, CA) and FITC-conjugated (Biolegend, San Diego, CA) antibodies, respectively. The ALDH1 activity was assessed with the ALDEFLUOR kit (Stemcell Technologies, Vancouver, Canada). All cells were analyzed by a BD Aria II flow cytometer.

2.6. Cell proliferation assays and cell cycle analysis

The cells were plated at a density of 1.0×10^4 cells per well in a 24-well plate. After seeding for 12 h, human recombinant IFN-γ (rhIFN-γ) was added at different concentrations (250 μg/ml, 500 μg/ml, 1000 μg/ml and 2000 μg/ml) every 3 days, and each concentration was repeated in triplicate. During the next 8 days, cells were harvested every 24 h and quantified with a hemocytometer. The dead cells were excluded by trypan blue staining.

To investigate the effect of IFN-γ treatment, cells subjected to various treatment lengths (0–8 days) and concentrations (250 μg/ml, 500 μg/ml, 1000 μg/ml, and 2000 μg/ml) were analyzed with PI staining for cell cycle phase distribution. To differentiate between G0 and G1 cell cycle phases, we performed Hoechst 33342 (Sigma) – Pyronin Y (PY; Sigma) staining.

2.7. Determination of cell viability and apoptosis

To test the sensitivity of PKH^{hi}, PKH^{low} and PKH^{neg} cells to Oxa, Oxa (10 μg/ml) was added after the cells were cultured in serum-free (SF) medium for 14 days. The percentage of viable cells was analyzed by FCM with 7-AAD staining (5 min, room temperature; BD Pharmingen).

To test the pro-apoptotic effects of IFN-γ and/or Oxa treatment on PKH^{hi}, PKH^{low} and PKH^{neg} cells *in vitro*, each subpopulation was sequentially treated with rhIFN-γ (1000 μg/ml) and/or Oxa (10 μg/ml) for 6 days. We also investigated pro-apoptotic effects *in vivo*. PKH26-stained cells (2×10^6) were injected s.c. into nude mice. The xenografts were palpable after 7 days, and then, rhIFN-γ (2×10^5 U/mouse/2 days) was injected i.p for 1 week, and saline was injected as a control. FCM analysis of Annexin V (BD Pharmingen)-7-AAD double staining was used to determine the percentage of apoptotic and viable cells. The pro-apoptotic effect of IFN-γon PKH^{hi}, PKH^{low} and PKH^{neg} cells was confirmed with the terminal deoxynucleotidyl trans-

ferase dUTP nick end labeling (TUNEL) technique with an *in situ* Cell Death Detection Kit FITC (Roche, Germany). All procedures strictly followed the manufacturer's instructions.

2.8. Determination of the half inhibitory concentration (IC_{50})

To determine the half growth inhibitory concentrations (IC_{50}) of IFN-γ on PKH^{hi}, PKH^{low} and PKH^{neg} cells, different subsets were sorted and seeded into 96-well plates, and the viable cells were evaluated with the CellTiter 96® AQueous Non-Radioactive Cell Proliferation Assay (MTS, Promega). All experimental procedures followed manufacturer's instruction. IC_{50} values were determined by plotting a linear regression curve.

2.9. Quantitative Reverse-Transcription Polymerase Chain Reaction (qRT-PCR)

Because of the extremely low amount of total RNA extraction, especially from the PKH^{hi} cells, we used the Taqman® PreAmp Cells to CT™ Kit (Life Technologies Co.) to overcome this limitation. The kit amplifies target genes utilizing a 10–14 PCR cycle and specific primers. Taqman assays of OCT4, Nanog, Nestin, Bmi1 and IFNRα/β were purchased from Applied Biosystems (Life Technologies Co.). All procedures strictly followed the manufacturer's instructions.

2.10. Immunofluorescence

Cells were fixed with 4% paraformaldehyde for 20 min, blocked in 5% normal goat serum and incubated with a primary antibody against Lgr5 or IRF-1 (4 °C, overnight), followed by Dylight488 conjugated goat anti-rabbit antibody incubation (37 °C, 1 h). After immunolabeling, cells were washed with PBS, stained with DAPI (Sigma, St. Louis, MO, USA), and then viewed under laser confocal microscope (LCM, Leica SP-5, Germany).

2.11. Western blot analysis

Western blot analysis was performed according to the previously reported protocol with some modifications [29]. Antibodies against JAK1, pshospho-JAK1 (Tyr1022/1023), JAK2, pshospho-JAK2 (Tyr1007), STAT1, pshospho-STAT1 (Tyr701) and IRF-1 were obtained from Cell Signaling Biotechnology (Danvers, MA, USA).

2.12. In vivo tumorigenic assay and chemotherapeutic study

All mice were bred in defined conditions at the Laboratory Animal Research Center of Zhejiang Chinese Medicine University with the permission of the local animal care and ethical committee. To compare the tumor initiating capacity of the PKH^{hi}, PKH^{low} and PKH^{neg} cells, different amounts (1000, 5000, 25,000 cells) of each subset were obtained from tumor xenografts and then injected s.c. into nude mice to compare their tumor forming ability.

Two weeks after cell injection, all nude mice were randomly assigned to four groups ($n = 5$) with different treatments, including vehicle (saline, i.p.), Oxa (2 mg/kg/week, i.v.), rhIFN-γ (2×10^5 μg/mouse/2 days, i.p.), or Oxa (2 mg/kg/week, i.v.) combined with rhIFN-γ (2×10^5 μg/mouse/2 days, i.p.). All groups received treatment for 4 weeks, xenografts were then harvested and enzymatically disassociated to form single cells, and 25,000 or 5000 cells from each group ($n = 5$) were injected s.c. into nude mice for serial tumor formation assays. The observation time frame for tumor growth was up to 8 weeks. The tumor volumes were measured as length × width × width/2.

2.13. Statistical analysis

All data are presented as the means ± SD. Statistical analysis was performed with the SPSS 10.0 software package. A two-sided value of $P < 0.05$ was considered statistically significant.

3. Results

3.1. Label-retaining cancer cells, especially PKH^{hi} cells, exhibit stronger CSC-like capacities

To isolate cells with different fluorescent intensities, cells were stained with PKH26 in advance and then cultured in SF medium to yield spheroids or injected s.c. into nude mice for xenograft formation. Fourteen days later, either *in vitro* or *in vivo*, the cells exhibited a continuous gradient of fluorescence intensity; only a few cells retained a strong fluorescence intensity (PKH^{hi}, 0.87 ± 0.30%), whereas some cells retained less of the fluorescent label (PKH^{low}, 39.2 ± 11.58%), and the remaining cells completely quenched the label (PKH^{neg}, 58.2 ± 8.32%; Fig. 1A and B), which was attributed to self-renewal and subsequent cell division. Based on the hierarchy model of tumor formation, we postulate that these three populations are heterogeneous in terms of CSC-like properties.

We then determined whether the PKH^{hi} cells were in a quiescent state. For this purpose, Hoechst 33342 – Pyronin Y staining was performed to compare the G0 phase distributions in PKH^{hi}, PKH^{low} and PKH^{neg} cells. Our results showed that the majority of PKH^{hi} cells were in the G0 phase (78.07 ± 1.98%), whereas only a minority of the population of PKH^{low} and PKH^{neg} cells were in G0 phase (1.14 ± 0.48%, 1.87 ± 0.34%, respectively) (Fig. 1C, Supplementary Fig. S1A), which indicated that the PKH^{hi} population represented actual quiescent cells.

Because CSCs exhibit dominant self-renewal, chemoresistance and tumor-initiating capacities [27], we contrasted these properties among the three populations. In colony formation assays, PKH^{hi} cells (35.6 ± 6.39 colonies/100 cells) showed a much greater ability than both PKH^{low} (15.8 ± 4.89 colonies/100 cells) and PKH^{neg} cells (3.2 ± 1.3 colonies/100 cells) to form colonies (Fig. 1D, Supplementary Fig. S1B). In a tumorigenicity assay, the tumor-initiating capacity of PKH^{hi} cells was far stronger than both the PKH^{low} and PKH^{neg} cells; only 1000 PKH^{hi} cells could form xenografts in nude mice, while the tumor-initiating thresholds of the PKH^{low} and PKH^{neg} cells were approximately 5000 and 25,000 cells, respectively (Fig. 1E, Supplementary Table S2). Next, we used Oxaliplatin (Oxa), a first line chemotherapeutic drug for colon cancer treatment to investigate the chemoresistance ability of the three subpopulations. Our previous study showed that Oxa could enrich CSC-like cells [28]. In this study, we demonstrated that Oxa is effective when treating primary colon cancer cells *in vitro* (Supplementary Fig. S1C). The treatment could enrich the PKH^{hi} population by 33.75 ± 7.14-fold compared with the control group (Fig. 1F), while the percentage of viable cells in PKH^{low} and PKH^{neg} decreased significantly (data not shown). These results suggest that PKH^{hi} cells are especially resistant to conventional chemotherapy.

3.2. CSC markers and stemness-related genes are preferentially overexpressed in PKH^{hi} cells

Several cell surface markers, such as CD133+, CD44+/CD24+ and ALDH1+, have been used to identify colon CSCs in recent years [29–32]. Therefore, we investigated these markers in the three populations of P2 cells. It was remarkable that all markers were preferentially expressed in PKH^{hi} cells (CD133+, 57.5 ± 13.3%; CD44+/CD24+, 71.6 ± 11.8%; and ALDH1+, 16.3 ± 2.1%), but this expression greatly decreased when the label intensity decreased (PKH^{low} CD133+, 16.4 ± 3.3%; CD44+/CD24+, 27.8 ± 7.2%; ALDH1+, 3.7 ± 1.4%; PKH^{neg} CD133+, 1.5 ± 1.4%; CD44+/CD24+, and 4.7 ± 1.1%; ALDH1+, 0%; Fig. 2A). The other two primary colon cancer cell lines showed that PKH^{hi} cells possessed the greatest level of CSC markers, similar to that seen with P2 cells (Supplementary Fig. S1D).

Furthermore, we determined the expression level of four stemness-related genes, OCT4, Nanog, Bmi1 and Nestin [9], in the three subsets of cells. Although these genes could be detected in all three subsets of cells, the expression levels increased more dramatically in the PKH^{hi} population (Fig. 2B) compared with the other two cell subsets. However, the PKH^{low} population still significantly showed a higher expression level compared with the PKH^{neg} population (Fig. 2B). This trend strongly suggests that there is a hierarchical relationship among the three cell groups and that the PKH^{hi} population can thus be considered a distinct CSC subset, independent of the reported markers that define the CSC subpopulation.

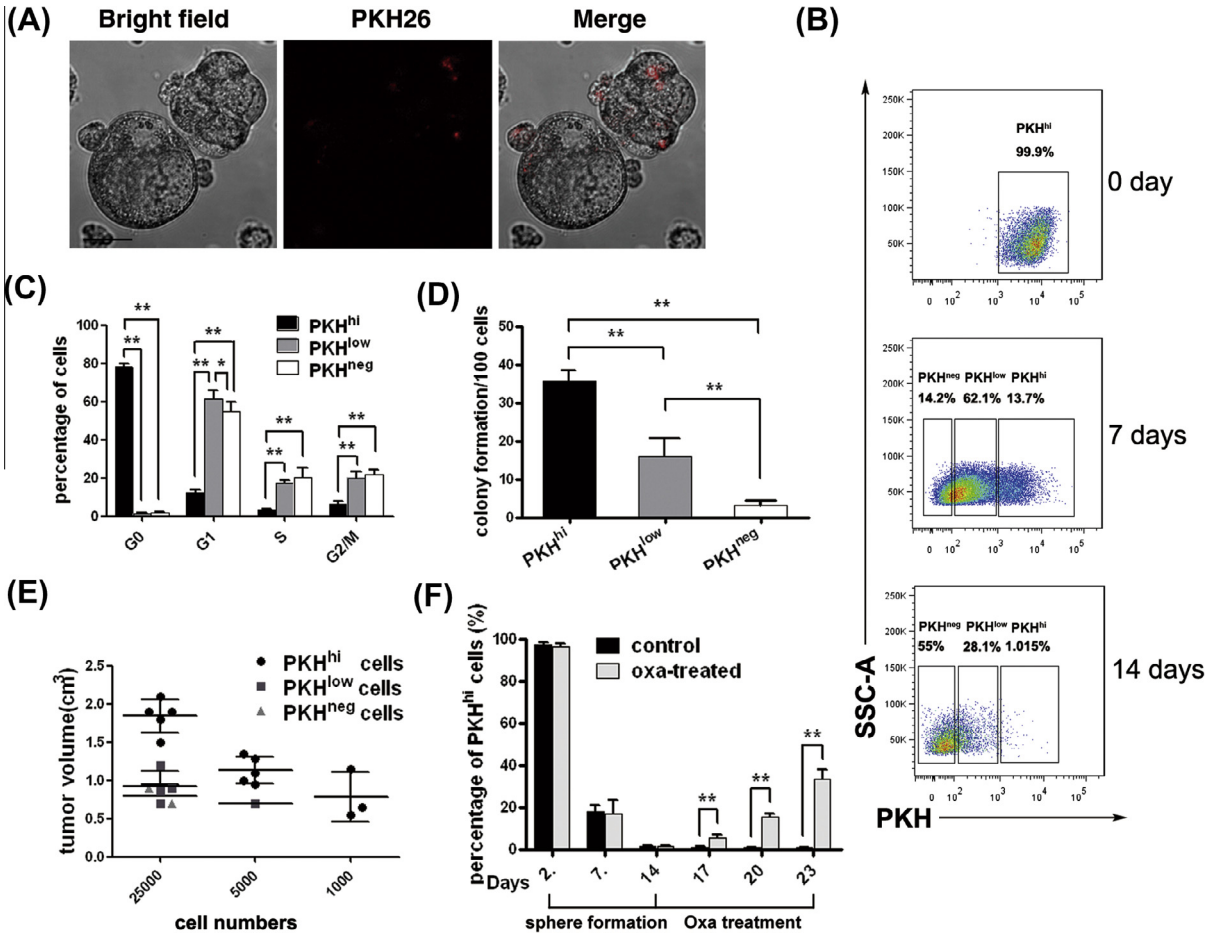

Fig. 1. Identification of LRCC and its CSC-like traits within primary colon cancer cells. (A) A colon sphere derived from PKH26-labeled cells. Scale bar = 100 μm. (B) PKH-labeled P2 cancer cells were seeded in SF culture conditions, and PKH intensity was detected by FCM on days 0, 7 and 14. (C) Cell cycle distributions of PKH^{hi}, PKH^{low} and PKH^{neg} cells. (D) Cells with different fluorescent intensities were seeded into soft agar to perform a colony formation assay. (E) Sorted PKH^{hi}, PKH^{low} and PKH^{neg} cells were injected s.c. into nude mice. The size of the xenotransplanted tumors in different mouse groups was measured. (F) Oxa was added into the colon sphere culture system on day 14, and the percentage of the PKH^{hi} population in total live cells (7-AAD-) under each Oxa treatment was assessed on days 17, 20 and 23. The data are shown as one typical result from 3 independent experiments with similar results or as the mean ± SD of 3 independent experiments. $^{*}p < .05$; $^{**}p < .01$.

3.3. Lgr5+ and PKH^{hi} cells are two distinct populations and Lgr5+ cells could be derived from PKH^{hi} cells

Although the above evidence indicates the extreme stemness of LRCCs in colon cancer cells, several studies in the literature report that there is another subpopulation of CSCs that exists, which is not in a quiescent state but a rapid cycling state [11,12,33]. Consequently, we first investigated the relationship between PKH^{hi} cells and Lgr5+ cells. P2 cells were labeled with PKH26 and cultured in SF medium for 14 days, and FCM analysis showed that approximately 10% of cells were Lgr5 positive; nearly all P2 cells were Ki67 positive but were not included in the PKH^{hi} subset (Fig. 2D and E). Next, we sorted the PKH^{hi} cells and seeded the cells on chamber slides for series confocal observation. Interestingly, we observed that PKH^{hi} cells expressed very weak Lgr5 level initially, but during cell division and differentiation, the Lgr5 level gradually increased and migrated from the cytoplasm to the cell membrane (Fig. 2F). This is the first study to report that a relationship exists between LRCCs and Lgr5+ cells, which are known to be two CSC subpopulations with different cell cycle properties. This result indicates that Lgr5+ cells could be derived from LRCCs. Therefore, the question of how to eradicate quiescent cancer stem cells could be an important issue for future research.

3.4. IFN-γ treatment selectively exerts pro-apoptosis effects on PKH^{hi} cells

Accumulating evidence suggests that dendritic cells can eradicate CSC-like cells by enhancing IFN-γ secretion [34,35], implying that CSCs are not resistant to IFN-γ. We first determined whether IFN-γ functions to prevent sphere formation in SF medium. Interestingly, we observed that spheroid formation was greatly inhibited with only 250 μg/ml rhIFN-γ, whereas a higher dose (1000 μg/ml) resulted in complete loss of the spheroids (Fig. 3A). These results strongly indicate that IFN-γ can reduce the self-renewal property of CSC-like cells.

Because PKH^{hi}, PKH^{low} and PKH^{neg} cells have various CSC-like capacities, we studied the apoptotic effects of IFN-γ treatment on all three cell populations. Using P2 cells, the three populations were isolated from spheroids and treated with rhIFN-γ (1000 μg/ml). The results showed strikingly different responses of the PKH^{hi}, PKH^{low} and PKH^{neg} cells to IFN-γ treatment. We set the percentage of viable cells prior to treatment as a control; IFN-γ treatment exerted a significant pro-apoptotic effect on the PKH^{hi} subsets (3 days of treatment, 38.57 ± 4.12%; 6 days of treatment, 13.8 ± 2.95% treatment), whereas PKH^{low} subsets revealed a more muted response (3 days of treatment, 77.2 ± 6.90%; 6 days of treatment, 47.2 ± 4.03%), and PKH^{neg} cells seemed to be the most resistant

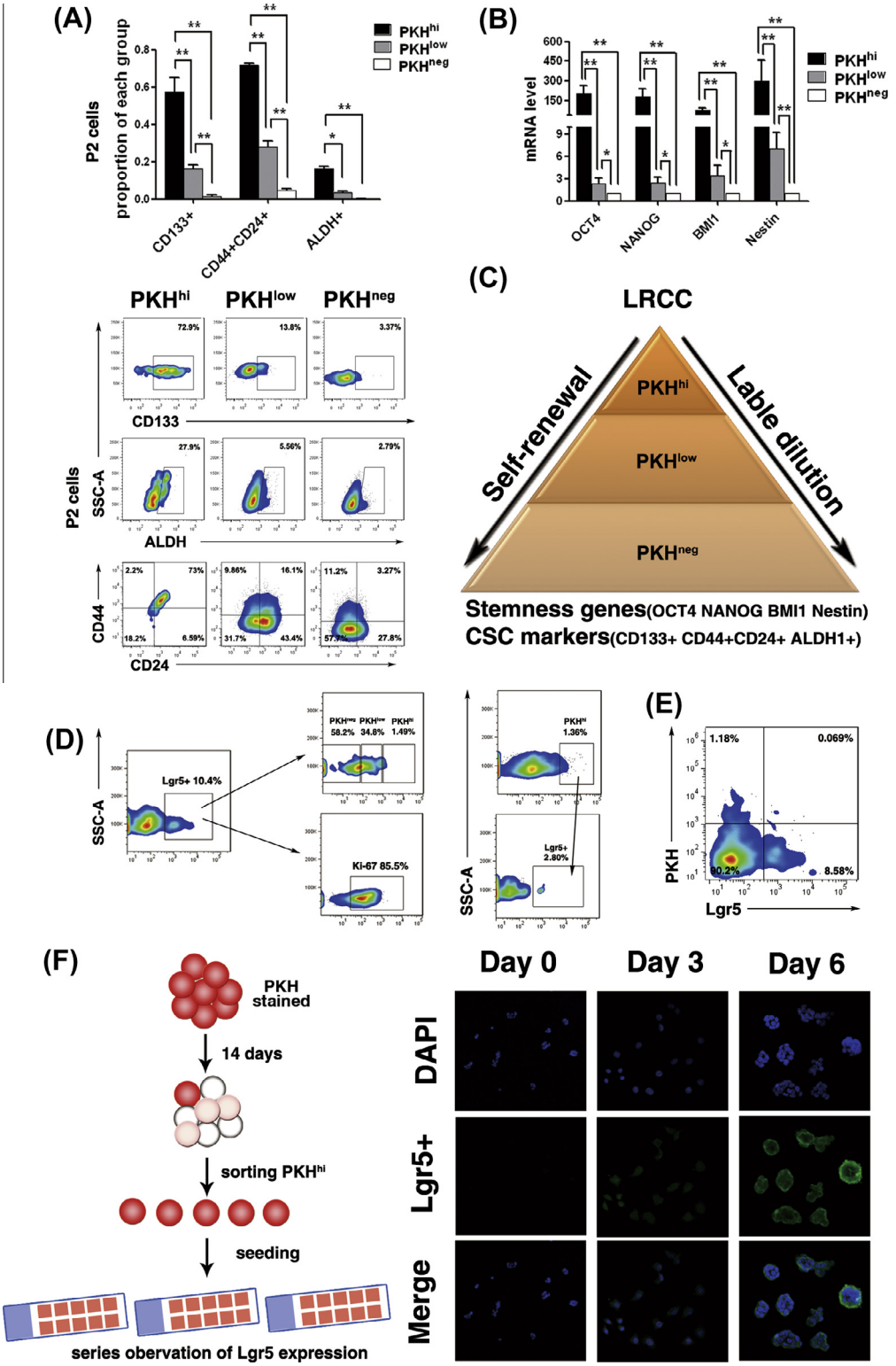

Fig. 2. Higher expression levels of colon CSC markers and stemness-related genes in PKH^{hi} cells. (A) FCM analyses of colon CSC-related markers (CD44+CD24+, CD133+ and ALDH1+) in three populations of P2 cancer cells. (B) Expression of four stemness-related genes in three subsets as detected by qRT-PCR. (C) Schematic illustration of CSC markers and stemness-related genes that decrease during the self-renewal process and label dilution. (D) FCM analyses of PKH^{hi}, PKH^{low} and PKH^{neg} subsets distribution within Lgr5+ cells and ki67 expression of Lgr5+ cells; FCM analyses of Lgr5+ cells which is gated on PKH^{hi} subset. (E) FCM analyses both gated on PKH^{hi} and Lgr5+ cells. (F) PKH^{hi} cells are sorted and seeded on chamber slides, then Lgr5 expression are observed every three days. The data are shown as one typical result from 3 independent experiments with similar results or as the mean ± SD of 3 independent experiments. $^{*}p < .05$; $^{**}p < .01$.

to the IFN-γ treatment (3 days of treatment, 87.13 ± 5.15%; 6 days of treatment, 72.0 ± 4.41%, Fig. 3B). The TUNEL assay also confirmed the selective pro-apoptotic effect of the IFN-γ treatment on the PKH^{hi} subset (Supplementary Fig. S2A). In addition, we also demonstrated that the specific pro-apoptotic effect of the IFN-γ treatment on PKH^{hi} cells was dose-dependent (Fig. 3E), and the half

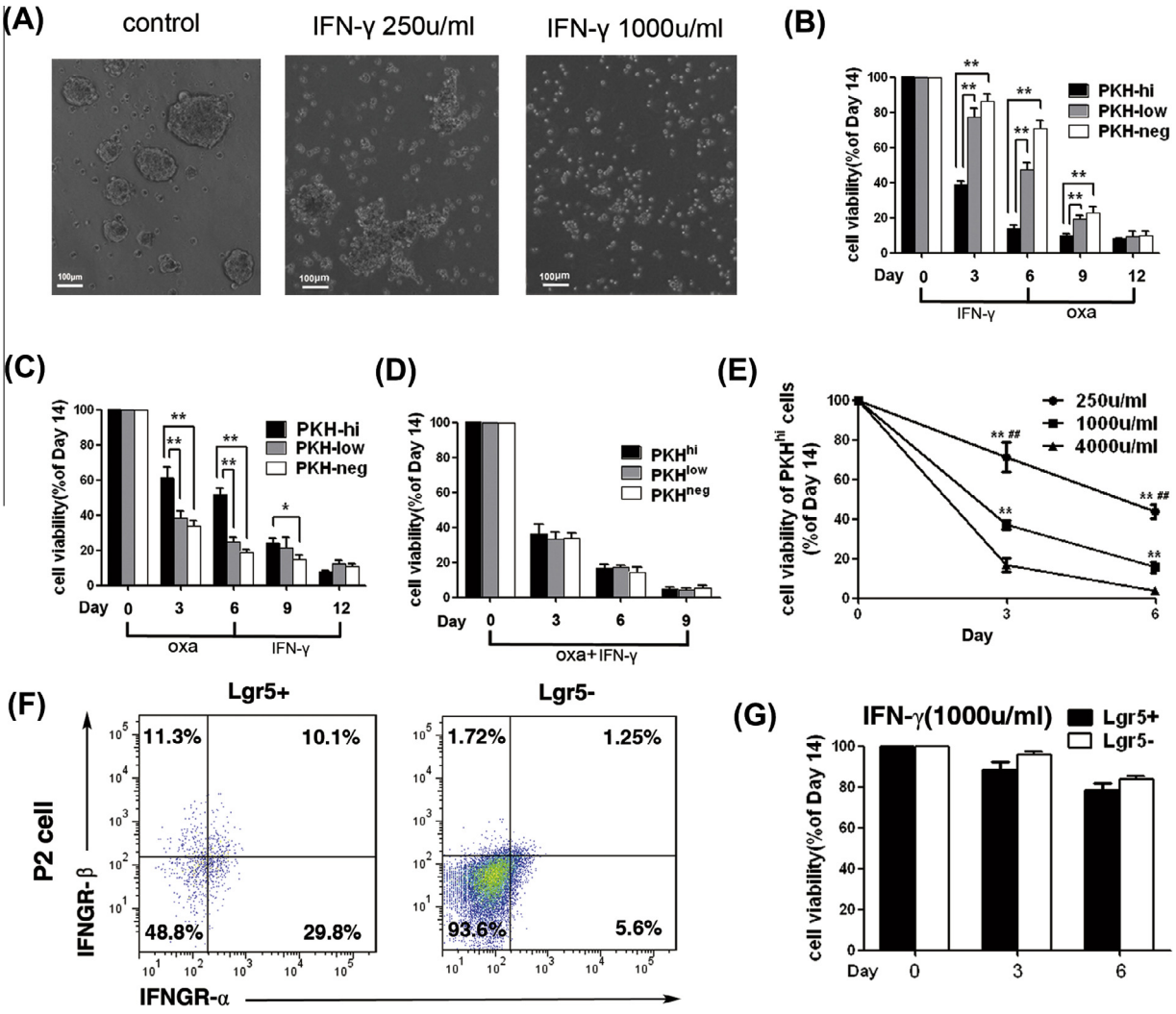

Fig. 3. IFN-γ specifically induces apoptosis in the PKH^{hi} cells. (A) Spheroid formation assay of P2 cancer cells with rhIFN-γ treatments (250 μ/ml, 1000 μ/ml). (B–D): After spheroid formation, PKH^{hi}, PKH^{low} and PKH^{neg} cells were sorted and then treated by IFN-γ and Oxa sequentially. Cell viability was measured on days 0, 3, 6, 9 and 12. (B) Cells were given rhIFN-γ (1000 μ/ml) for 6 days, and then received Oxa (10 μg/ml) treatment for another 6 days. (C) Cells were given Oxa (10 μg/ml) for 6 days, and then co-incubated with rhIFN-γ (1000 μ/ml) for another 6 days. (D) Cells were treated with Oxa (10 μg/ml) and rhIFN-γ (1000 μ/ml) together. $^{*}p < .05$; $^{**}p < 0.01$. (E) PKH^{hi} cells were cultured in the presence of IFN-γ at different concentrations and their viability was measured using FCM on day 3 and day 6. (F) FCM analyses of IFN-γ receptors expression on Lgr5+ and Lgr5− cells. (G) After spheroid formation, Lgr5+ and Lgr5− cells were sorted and then treated with rhIFN-γ (1000 μ/ml) for 6 days. The data are shown as one typical result from 3 independent experiments with similar results or as the mean ± SD of 3 independent experiments. $^{\#\#}$Indicates *vs.* 1000 μ/ml $p < .01$; **indicates *vs.* 4000 μ/ml $p < .01$.

inhibitory concentration (IC_{50}) of IFN-γ-treated PKH^{hi} cells was much lower than that in IFN-γ-treated PKH^{low} and PKH^{neg} cells (Fig. S2B). Similar results were confirmed in P1, P3, HT29 and HCT116 cells (Supplementary Fig. S3A).

In a subsequent experiment, we assessed the effect of IFN-γ treatment on the total population of colon cancer cells, and as expected, IFN-γ treatment suppressed cellular proliferation in a dose-dependent manner (Supplementary Fig. S4A). In addition, PI staining revealed both a moderate cell cycle arrest and a pro-apoptotic function of IFN-γ, but only the pro-apoptotic function of IFN-γ was enhanced with increasing concentrations (Supplementary Fig. S4B). Considering the results above, we speculated that IFN-γ mainly exerts pro-apoptotic effects on the colon cancer cells.

Next, we verified the *in vivo* effect of IFN-γ treatment on PKH^{hi} cells. After 7 days of treatment, the percentage of viable cells in the PKH^{hi} cell subset significantly decreased (51.17 ± 11.72%) in contrast to the control group, but the viability of the PKH^{low} and PKH^{neg} cells was considerably unaffected (PKH^{low} 77.5 ± 7.72%; PKH^{neg} 89.07 ± 5.44%, Fig. 5A). These results clearly suggest that IFN-γ treatment selectively induces apoptosis of the PKH^{hi} population and that its effect greatly decreases with label quenching.

3.5. PKH^{hi} cells are specifically sensitive to IFN-γ treatment due to a higher level of IFN-γ receptors

Given the different responses to IFN-γ treatment among the PKH^{hi}, PKH^{low} and PKH^{neg} cells, we sought to determine the detailed mechanism behind these responses. A previous study demonstrated that a high level of functional IFN-γR could rapidly activate JAK–Stat1–IRF1 signaling to induce apoptosis, whereas low levels of IFN-γR were not sufficient [36]. Thus, we evaluated IFN-γR expression in the PKH^{hi}, PKH^{low} and PKH^{neg} cells. The FCM analyses highlighted the different IFN-γRα and IFN-γRβ expression in the three cell populations; expression of both the two IFN-γR subunits was considerably higher in the PKH^{hi} subset but lower in the PKH^{low} and PKH^{neg} subsets (Fig. 4A, Supplementary Fig. S3A). Because the expression of IRF-1 was closely related to the IFN-γR levels after IFN-γ treatment [36], we studied the expression of IRF-1 after rhI-

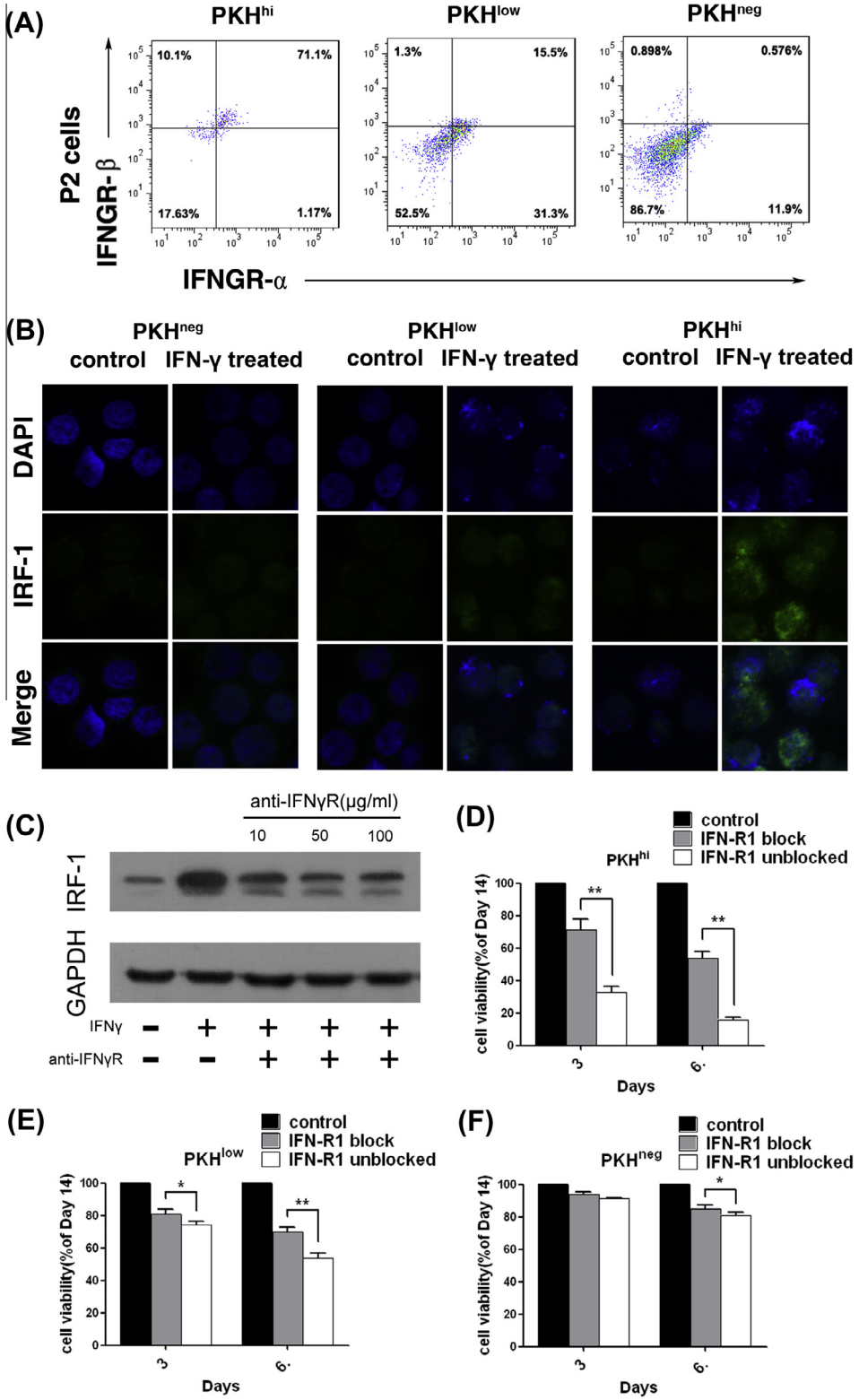

Fig. 4. Higher levels of IFN-γ receptors on PKH^{hi} cells determine their sensitivity to IFN-γ treatment. (A) Expression of IFN-γRα and IFN-γRβ proteins in PKH^{hi}, PKH^{low} and PKH^{neg} cells. (B) Immunostaining of IRF-1 (green) in PKH^{hi}, PKH^{low} and PKH^{neg} cells after rhIFN-γ (1000 μ/ml) treatment for 6 days. Nuclei were counterstained with DAPI. (C) Cells were pre-cultured with or without the neutralizing anti- IFN-γRα antibody (10 μg/ml) then treated with rhIFN-γ (1000 μ/ml). IRF-1 expression was detected by western blot. An isotype-indicated control was used along with the antibody to IFN-γRα. (D–F) Cells were pre-cultured with or without the neutralizing anti- IFN-γR antibody then treated with rhIFN-γ (1000 μ/ml). The cell viability of PKH^{hi} (E), PKH^{low} (F) and PKH^{neg} (G) cells was measured by FCM on day 3 and day 6. The data are shown as one typical result from 3 independent experiments with similar results or as the mean ± SD of 3 independent experiments. $^{*}p < .05$; $^{**}p < .01$.

FN-γ (1000 μg/ml) treatment. We found that the PKH^{hi} cells had the highest expression of IRF-1, whereas the PKH^{low} and PKH^{neg} cells showed a slight upregulation (Fig. 4B).

To verify that the differential expression of the IFN-γR was the dominating factor that gave rise to the various responses after IFN-γ treatment, we blocked IFN-γR and observed the changes. Because the two IFN-γ receptor subunits are indispensable—the IFN-γRα chain is important for binding and the IFN-γRβ chain is important for signal transduction—in our study, we blocked IFN-γRα using its neutralizing antibody. Cells were pre-incubated with anti-human IFN-γRα antibody (10 μg/ml) for 30 min, and it was shown that the upregulation of IRF-1 induced by IFN-γ was greatly inhibited (Fig. 4C). Additionally, the specific apoptotic function of IFN-γtreatment on the PKH^{hi} cells was neutralized (Fig. 4D), which further supports our hypothesis. All the above evidence strongly suggests that increased IFN-γR expression in the PKH^{hi} subset plays a key role in its sensitivity to the apoptotic function induced by IFN-γ.

Furthermore, we analyzed the IFN-γR expression level in Lgr5+ and Lgr5− cells. The results showed a higher level of both IFN-γRα and IFN-γRβ expression in Lgr5+ cells (Supplementary Fig. S3B); however, no differences in IFN-γR expression as a result of IFN-γ treatment were observed between these two populations (Fig. 3F and G).

3.6. IFN-γ functions synergistically with Oxaliplatin to eliminate both LRCCs and non-LRCCs

Based on the above results, we performed a sequential treatment using Oxa and/or IFN-γ. Cells from the different populations were first treated with Oxa (10 μg/ml) and then co-incubated for another 6 days with rhIFN-γ (1000 μ/ml). FCM analyses demonstrated that Oxa-resistant PKH^{hi} cells underwent apoptosis with IFN-γ treatment (Fig. 3C). When the treatment order was reversed, the majority of the PKH^{hi} cells were dead after IFN-γ treatment, but the majority of the PKH^{hi} cells survived after Oxa treatment. However, most of the PKH^{low} and PKH^{neg} cells were viable during the IFN-γ incubation but were efficiently killed by Oxa treatment (Fig. 3B). When treated with a combination of Oxa and IFN-γ, the PKH^{hi}, PKH^{low} and PKH^{neg} cells were eliminated simultaneously (Fig. 3D).

To confirm this effect of combined therapy *in vivo*, we used a serial transplantation model. Mice carrying xenografts were randomly divided into four groups that received different treatments for 1 month. Compared with the monotherapy group, combined

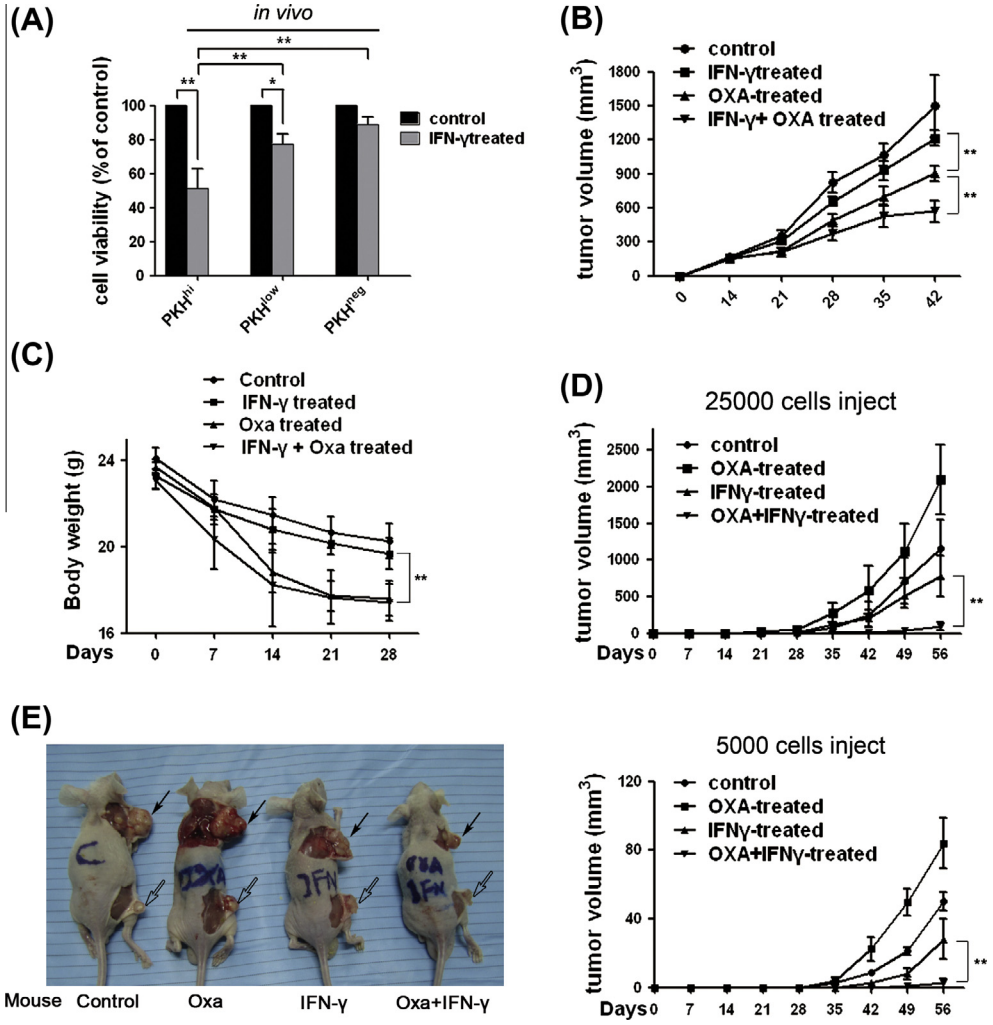

Fig. 5. IFN-γ exerts synergistic effects with Oxaliplatin on cancer cells *in vivo*. (A) *In vivo* detection of cell viability with rhIFN-γ (1000 μ/ml) treatment for 7 days. (B and C) 5×10^6 P2 cancer cells were injected s.c. into nude mice, and 2 weeks later, the tumor-bearing mice were administered Oxa (2 mg/kg/week, i.v.), rhIFN-γ (2×10^5 μ/mouse/2 days, i.p.), or Oxa (2 mg/kg/week, i.v.) combined with rhIFN-γ (2×10^5 μ/mouse/2 days, i.p.). The tumor size (B) and body weight of the mice (C) were measured every 7 days. (D and E) Indicated numbers of cells from tumors with different month-long treatments, as described in (B), injected s.c. into nude mice for serial tumor formation. (D) Tumor growth curve of indicated cell numbers. (E) Representative image of tumor formation in nude mice; the solid arrow indicates 2.5×10^4 cells per injection and the hollow arrow indicates 5×10^3 cells. Each data point represents the mean ± SD of $n = 6$ mice. $^{*}p < .05$; $^{**}p < .01$.

Table 1
Series tumor formation incidence of P2 cancer cells from the exnografts with various treatments.

Pre-treated cell types	No. of cells injected	Tumor incidence	Latency(days)
Control	2.5×10^4	5/5	28
	5×10^3	5/5	35
Oxa	2.5×10^4	5/5	21
	5×10^3	5/5	28
IFN-γ	2.5×10^4	5/5	28
	5×10^3	3/5	42
Oxa + IFN-γ	2.5×10^4	3/5	42
	5×10^3	1/5	49

Abbreviation: Oxa, Oxaliplatin.

administration of IFN-γ and Oxa showed a greater effect on tumor growth inhibition. However, in contrast to the control group, the IFN-γ monotherapy group showed a slight tumor repressive function (Fig. 5B). Because of animal safety concerns, we ensured that all control animals and IFN-γ monotherapy animals were viable during the treatments and exhibited similar body weights (Fig. 5C). However, two animals died, and the remaining mice lost a considerable amount of weight in both the combination therapy and Oxa monotherapy groups (Fig. 5C), suggesting that the IFN-γ did not augment the toxicity of Oxaliplatin.

Because of the synergistic anti-cancer effects of IFN-γ and Oxa, which could eliminate LRCCs and non-LRCCs together *in vitro*, we compared the tumor-initiating capacity of the cells from the xenograft tumor after the different treatments described above. Tumors from each therapy group were dissociated into single cells and injected into the flanks of mice with different indicated cell numbers. Consequently, in the second xenograft formation assay, cancer cells from the Oxa-treated group formed tumors in all mice at 2.5×10^4 cells/injection and 5×10^3 cells/injection, and these tumors possessed the largest tumor volumes, which could be attributed to the enrichment of the CSCs by chemotherapy. However, IFN-γ monotherapy resulted in a moderate decrease in tumor formation capacity, which was observed in 5/5 and 3/5 nude mice using the same cell numbers. Meanwhile, compared with the other groups, the combination therapy significantly reduced the tumor formation ratio and tumor volume (Fig. 5D and E, Table 1). Altogether, these data suggest that IFN-γ treatment combined with chemotherapy could profoundly enhance anti-tumor effects and decrease the capacity for serial tumor formation.

4. Discussion

LRCCs have been previously defined according to the label staining assay and compose 0.4–3% of all cells in solid tumors; however, the amount of time spent to isolate quiescent cancer cells varied in different tissue types (6 days – 6 weeks) [9,37–44], which suggests that the cell division time differs among various cancer cells but that the percentage of LRCCs remains relatively stable. In our study, we found that the fluorescence-quenching rate, which represented the cellular division time, was similar both *in vivo* and in SF culture conditions within a 2-week timeframe. However, the LRCCs rapidly lost fluorescence *in vivo* after 16–18 days, but the fluorescence remained relatively stable *in vitro* for 4 weeks. A possible reason for this difference is that the overgrowth of the xenograft caused a nutrition deficiency and resulted in tumor necrosis *in vivo*, which caused the dormant CSCs to proliferate and replenish the lost cells, resulting in a rapid loss of fluorescence. Based on this phenomenon and our hypothesis, LRCCs were isolated 2 weeks after staining for subsequent study.

Although quiescent cells in the normal intestinal tract have attracted much attention recently [45–48], the evidence of LRCCs existence in colon cancer is very limited. Xin et al. [37] showed that LRCCs have increased CSC-like features compared with non-LRCCs in gastrointestinal cancers. We obtained similar results by demonstrating that the majority of PKH^{hi} cells were quiescent. We also differentiated cells into three populations, and nearly all CSC-like properties were closely associated with fluorescence intensity, which was especially high in the PKH^{hi} subset. It has also been found that in ovarian cancer the expression of both stemness-related genes and CSC markers was enriched in the PKH^{hi} subset but lost in the PKH^{neg} subset [9]. To further elucidate the relationship between CSC markers (CD133+, CD44+/CD24+, ALDH1+) and label intensity, we noted that none of these CSC markers were definitively useful in identifying the PKH^{hi} population. In other words, the CSC markers and LRCCs overlapped or enriched each other. Additionally, expression of these markers could be detected in the PKH^{low} and PKH^{neg} populations. Based on the theory of stochastic equilibrium between CSC-like and non-CSC-like cells [49], we speculated that the cells with low label retention may persist but that they may have a much lower tumor-initiating capacity. However, increasing evidence has shown that a subpopulation of rapid cycling cells in the intestinal tract also exhibit stem cell traits, both in normal tissues and cancer lesions. Yan et al. [11] found that Bmi1 and Lgr5 could independently identify long-lived multipotent intestinal stem cells by lineage tracing in mice; the former represents quiescent subpopulations, and the latter represents mitotically active subpopulations. Although both quiescent and mitotically active subpopulations displayed the ability to rebuild the intestinal structure, after the epithelium was injured by radiation, only the quiescent ISCs could quickly proliferate to facilitate epithelium regeneration. Additionally, the quiescent subpopulations give rise to the Lgr5+ cells. Recently, Kobayashi et al. [12] reported that Lgr5+ colon cancer stem cells could interconvert with the non-cycling 'Lgr5−' state after chemodrug treatment, but the original relationship between quiescent and rapid cycling CSCs was not specified. Here, we are the first to report that LRCCs and Lgr5+ cells are two distinct subpopulations in colon cancer cells and that LRCCs could give rise to Lgr5+ cells during proliferation. Altogether, these data indicate that LRCCs represent a distinct cell population and that they could be considered putative, novel stem-like cancer cells. Moreover, the fact that the CSC-like traits of LRCCs gradually decreased along with the fluorescence dilution strongly supports the hierarchical model of the CSC theory. More recently, the lineage tracing technique has been applied to demonstrate that the hierarchical organization of tumors is driven by CSCs, especially by quiescent cancer cells [10,50,51]. Although increasing evidence stresses the importance of LRCCs in tumor initiation, to the best of our knowledge, a method of eliminating LRCCs or quiescent cancer cells has not yet been described.

We demonstrated that slow-cycling populations, PKH^{hi} cells, were especially sensitive to IFN-γ treatment, the only member of the Type II interferon family, resulting in dramatic apoptosis both *in vitro* and *in vivo*, whereas PKH^{low} and PKH^{neg} cells were less responsive. This interesting result led us to investigate the mechanism behind the difference in apoptosis levels.

Because we showed that the Jak-Stat1 pathway in our primary cell lines was intact (Supplementary Fig. S3C), we hypothesized that the different responses to IFN-γ treatment among the PKH^{hi}, PKH^{low} and PKH^{neg} populations might contribute to their IFN-γR expression levels. In fact, FCM analyses confirmed our speculation that the IFN-γR level was much higher in PKH^{hi} cells than in the other two subsets. Based on the core position of IRF-1 in IFN-γ-induced apoptosis [36,52,53], we assessed the expression level of IRF-1 in the three populations after IFN-γ treatment and found that its expression corresponded well with the different IFN-γR levels in the three cellular subsets. Moreover, blocking IFN-γRα greatly inhibited the apoptotic function of IFN-γ in PKH^{hi} cells, which could be further evidence that the IFN-γR levels are indicative of cellular fate.

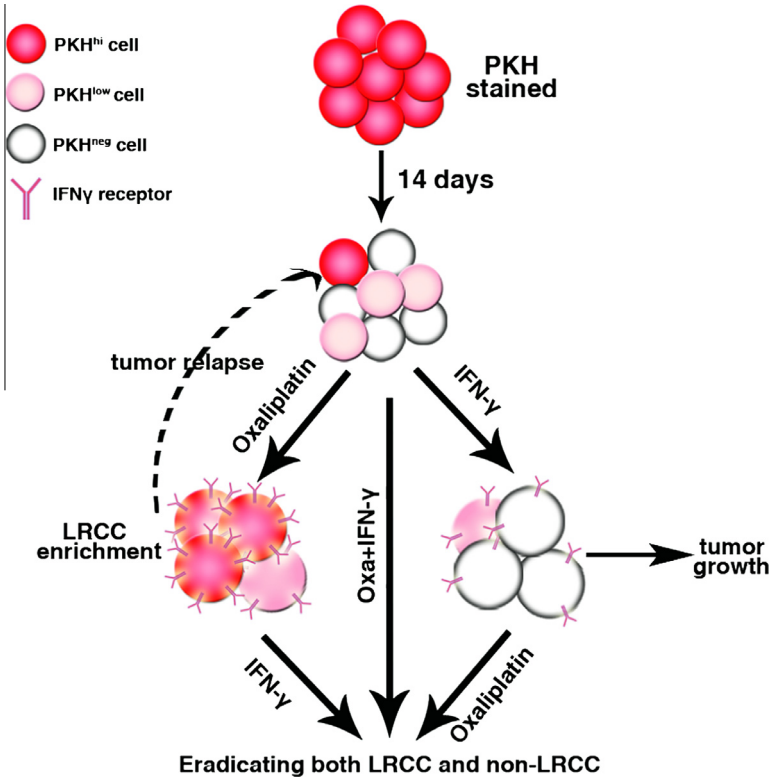

Fig. 6. Schematic illustration of IFN-γ combined with Oxaliplatin to eradicate both LRCC and non-LRCC.

Additionally, previous phases I–III trials have already demonstrated that combination therapy of IFN-γ with cisplatin and cyclophosphamide is an effective first-line treatment for patients with advanced ovarian cancer, with an improvement in progression-free survival [20,54] and well-tolerated side effects. However, the exact effect of IFN-γ combined with platinum-based treatment in colon cancer is still unclear. Here, we first report that combination therapy with Oxa and IFN-γ can synergistically eradicate LRCCs and non-LRCCs (Fig. 6), which has implications for future clinical translation.

Our finding that the expression of IFN-γR rapidly decreases when cells undergo self-renewal and proliferation partly explains the mechanism of cancer cell immune escape. However, we acknowledge that the mechanism behind the different IFN-γR expression levels in the three populations is still undetermined. The hierarchical relationship among the three subsets may be due to genetic or epigenetic modulation occurring along with the self-renewal process. Elucidating this mechanism could provide a solid foundation for clinical applications and even provide a potential novel anti-cancer approach.

Conflict of Interest

None.

Acknowledgments

We thank Dr. Ke Wang for his excellent work in the primary colon cancer cells preparation, and the support of core faculties of Zhejiang University, School of Medicine. This study is support by the National Natural Science Foundation of China (No. 91019005), Zhejiang Province and Ministry of Health (Grant No. 2012ZDA021), Nature science foundation of Zhejiang Province (Grant No. Y2110034; Y2100414) and major plan of Zhejiang Science and Technology Department (Grant No. 2011c13034~1).

Appendix A. Supplementary material

Supplementary data associated with this article can be found, in the online version, at http://dx.doi.org/10.1016/j.canlet.2013.04.029.

References

[1] T.M. Yeung, S.C. Gandhi, J.L. Wilding, R. Muschel, W.F. Bodmer, Cancer stem cells from colorectal cancer-derived cell lines, Proceedings of the National Academy of Sciences of the United States of America 107 (2010) 3722–3727.
[2] S.P. Lin, Y.T. Lee, S.H. Yang, S.A. Miller, S.H. Chiou, M.C. Hung, S.C. Hung, Colon cancer stem cells resist antiangiogenesis therapy-induced apoptosis, Cancer Letters 328 (2013) 226–234.
[3] S.V. Shmelkov, J.M. Butler, A.T. Hooper, A. Hormigo, J. Kushner, T. Milde, R. St Clair, M. Baljevic, I. White, D.K. Jin, A. Chadburn, A.J. Murphy, D.M. Valenzuela, N.W. Gale, G. Thurston, G.D. Yancopoulos, M. D'Angelica, N. Kemeny, D. Lyden, S. Rafii, CD133 expression is not restricted to stem cells, and both CD133+ and CD133− metastatic colon cancer cells initiate tumors, The Journal of Clinical Investigation 118 (2008) 2111–2120.
[4] C.H. Stuelten, S.D. Mertins, J.I. Busch, M. Gowens, D.A. Scudiero, M.W. Burkett, K.M. Hite, M. Alley, M. Hollingshead, R.H. Shoemaker, J.E. Niederhuber, Complex display of putative tumor stem cell markers in the NCI60 tumor cell line panel, Stem Cells 28 (2010) 649–660.
[5] W.Q. Nian, F.L. Chen, X.J. Ao, Z.T. Chen, CXCR4 positive cells from Lewis lung carcinoma cell line have cancer metastatic stem cell characteristics, Molecular and Cellular Biochemistry 355 (2011) 241–248.
[6] R. Pang, W.L. Law, A.C. Chu, J.T. Poon, C.S. Lam, A.K. Chow, L. Ng, L.W. Cheung, X.R. Lan, H.Y. Lan, V.P. Tan, T.C. Yau, R.T. Poon, B.C. Wong, A subpopulation of CD26+ cancer stem cells with metastatic capacity in human colorectal cancer, Cell Stem Cell 6 (2010) 603–615.
[7] C.A. O'Brien, A. Kreso, P. Ryan, K.G. Hermans, L. Gibson, Y. Wang, A. Tsatsanis, S. Gallinger, J.E. Dick, ID1 and ID3 regulate the self-renewal capacity of human colon cancer-initiating cells through p21, Cancer Cell 21 (2012) 777–792.
[8] Y. Kamohara, N. Haraguchi, K. Mimori, F. Tanaka, H. Inoue, M. Mori, T. Kanematsu, The search for cancer stem cells in hepatocellular carcinoma, Surgery 144 (2008) 119–124.
[9] A.P. Kusumbe, S.A. Bapat, Cancer stem cells and aneuploid populations within developing tumors are the major determinants of tumor dormancy, Cancer Research 69 (2009) 9245–9253.
[10] J. Chen, Y. Li, T.S. Yu, R.M. McKay, D.K. Burns, S.G. Kernie, L.F. Parada, A restricted cell population propagates glioblastoma growth after chemotherapy, Nature (2012).

[11] K.S. Yan, L.A. Chia, X. Li, A. Ootani, J. Su, J.Y. Lee, N. Su, Y. Luo, S.C. Heilshorn, M.R. Amieva, E. Sangiorgi, M.R. Capecchi, C.J. Kuo, The intestinal stem cell markers Bmi1 and Lgr5 identify two functionally distinct populations, Proceedings of the National Academy of Sciences of the United States of America 109 (2012) 466–471.
[12] S. Kobayashi, H. Yamada-Okabe, M. Suzuki, O. Natori, A. Kato, K. Matsubara, Y.J. Chen, M. Yamazaki, S. Funahashi, K. Yoshida, E. Hashimoto, Y. Watanabe, H. Mutoh, M. Ashihara, C. Kato, T. Watanabe, T. Yoshikubo, N. Tamaoki, T. Ochiya, M. Kuroda, A.J. Levine, T. Yamazaki, LGR5-positive colon cancer stem cells interconvert with drug resistant LGR5-negative cells and are capable of tumor reconstitution, Stem Cells (2012).
[13] J. Wei, J. Barr, L.Y. Kong, Y. Wang, A. Wu, A.K. Sharma, J. Gumin, V. Henry, H. Colman, R. Sawaya, F.F. Lang, A.B. Heimberger, Glioma-associated cancer-initiating cells induce immunosuppression, Clinical Cancer Research: An Official Journal of the American Association for Cancer Research 16 (2010) 461–473.
[14] T. Schatton, U. Schutte, N.Y. Frank, Q. Zhan, A. Hoerning, S.C. Robles, J. Zhou, F.S. Hodi, G.C. Spagnoli, G.F. Murphy, M.H. Frank, Modulation of T-cell activation by malignant melanoma initiating cells, Cancer Research 70 (2010) 697–708.
[15] L. Moserle, S. Indraccolo, M. Ghisi, C. Frasson, E. Fortunato, S. Canevari, S. Miotti, V. Tosello, R. Zamarchi, A. Corradin, S. Minuzzo, E. Rossi, G. Basso, A. Amadori, The side population of ovarian cancer cells is a primary target of IFN-α antitumor effects, Cancer Research 68 (2008) 5658–5668.
[16] K. Yuki, A. Natsume, H. Yokoyama, Y. Kondo, M. Ohno, T. Kato, P. Chansakul, M. Ito, S.U. Kim, T. Wakabayashi, Induction of oligodendrogenesis in glioblastoma-initiating cells by IFN-mediated activation of STAT3 signaling, Cancer Letters 284 (2009) 71–79.
[17] G. Beatty, Y. Paterson, IFN-γ-dependent inhibition of tumor angiogenesis by tumor-infiltrating CD4+ T cells requires tumor responsiveness to IFN-γ, Journal of Immunology 166 (2001) 2276–2282.
[18] M. Chawla-Sarkar, D.J. Lindner, Y.F. Liu, B.R. Williams, G.C. Sen, R.H. Silverman, E.C. Borden, Apoptosis and interferons: role of interferon-stimulated genes as mediators of apoptosis, Apoptosis: An International Journal on Programmed Cell Death 8 (2003) 237–249.
[19] T.J. Brown, M.N. Lioubin, H. Marquardt, Purification and characterization of cytostatic lymphokines produced by activated human T lymphocytes. Synergistic antiproliferative activity of transforming growth factor beta 1, interferon-gamma, and oncostatin M for human melanoma cells, Journal of Immunology 139 (1987) 2977–2983.
[20] C. Marth, G.H. Windbichler, H. Hausmaninger, E. Petru, K. Estermann, A. Pelzer, E. Mueller-Holzner, Interferon-gamma in combination with carboplatin and paclitaxel as a safe and effective first-line treatment option for advanced ovarian cancer: results of a phase I/II study, International Journal of Gynecological Cancer: Official Journal of the International Gynecological Cancer Society 16 (2006) 1522–1528.
[21] L. Wall, F. Burke, J.F. Smyth, F. Balkwill, The anti-proliferative activity of interferon-gamma on ovarian cancer: in vitro and in vivo, Gynecologic Oncology 88 (2003) S149–S151.
[22] K. Matsushita, T. Takenouchi, H. Shimada, T. Tomonaga, H. Hayashi, A. Shioya, A. Komatsu, H. Matsubara, T. Ochiai, Strong HLA-DR antigen expression on cancer cells relates to better prognosis of colorectal cancer patients: possible involvement of c-myc suppression by interferon-gamma in situ, Cancer Science 97 (2006) 57–63.
[23] K. Schroder, P.J. Hertzog, T. Ravasi, D.A. Hume, Interferon-gamma: an overview of signals, mechanisms and functions, Journal of Leukocyte Biology 75 (2004) 163–189.
[24] J. George, N.L. Banik, S.K. Ray, Combination of hTERT knockdown and IFN-γ treatment inhibited angiogenesis and tumor progression in glioblastoma, Clinical Cancer Research: An Official Journal of the American Association for Cancer Research 15 (2009) 7186–7195.
[25] R. Janardhanan, N.L. Banik, S.K. Ray, N-(4-Hydroxyphenyl) retinamide induced differentiation with repression of telomerase and cell cycle to increase interferon-gamma sensitivity for apoptosis in human glioblastoma cells, Cancer Letters 261 (2008) 26–36.
[26] J. George, N.L. Banik, S.K. Ray, Knockdown of hTERT and concurrent treatment with interferon-gamma inhibited proliferation and invasion of human glioblastoma cell lines, The International Journal of Biochemistry and Cell Biology 42 (2010) 1164–1173.
[27] N.A. Lobo, Y. Shimono, D. Qian, M.F. Clarke, The biology of cancer stem cells, Annual Review of Cell and Developmental Biology 23 (2007) 675–699.
[28] K. Wang, L. Liu, T. Zhang, Y.L. Zhu, F. Qiu, X.G. Wu, X.L. Wang, F.Q. Hu, J. Huang, Oxaliplatin-incorporated micelles eliminate both cancer stem-like and bulk cell populations in colorectal cancer, International Journal of Nanomedicine 6 (2011) 3207–3218.
[29] Y.K. Wang, Y.L. Zhu, F.M. Qiu, T. Zhang, Z.G. Chen, S. Zheng, J. Huang, Activation of Akt and MAPK pathways enhances the tumorigenicity of CD133+ primary colon cancer cells, Carcinogenesis 31 (2010) 1376–1380.
[30] L. Lin, A. Liu, Z. Peng, H.J. Lin, P.K. Li, C. Li, J. Lin, STAT3 is necessary for proliferation and survival in colon cancer-initiating cells, Cancer Research 71 (2011) 7226–7237.
[31] E.H. Huang, M.J. Hynes, T. Zhang, C. Ginestier, G. Dontu, H. Appelman, J.Z. Fields, M.S. Wicha, B.M. Boman, Aldehyde dehydrogenase 1 is a marker for normal and malignant human colonic stem cells (SCs) and tracks SC overpopulation during colon tumorigenesis, Cancer Research 69 (2009) 3382–3389.
[32] L. Vermeulen, M. Todaro, F. de Sousa Mello, M.R. Sprick, K. Kemper, M. Perez Alea, D.J. Richel, G. Stassi, J.P. Medema, Single-cell cloning of colon cancer stem cells reveals a multi-lineage differentiation capacity, Proceedings of the National Academy of Sciences of the United States of America 105 (2008) 13427–13432.
[33] V. Jaks, N. Barker, M. Kasper, J.H. van Es, H.J. Snippert, H. Clevers, R. Toftgard, Lgr5 marks cycling, yet long-lived, hair follicle stem cells, Nature Genetics 40 (2008) 1291–1299.
[34] Q. Xu, G. Liu, X. Yuan, M. Xu, H. Wang, J. Ji, B. Konda, K.L. Black, J.S. Yu, Antigen-specific T-cell response from dendritic cell vaccination using cancer stem-like cell-associated antigens, Stem Cells 27 (2009) 1734–1740.
[35] Z.Y. Xiao, H. Tang, Z.M. Xu, Z.J. Yan, P. Li, Y.Q. Cai, X.D. Jiang, R.X. Xu, An experimental study of dendritic cells transfected with cancer stem-like cells RNA against 9L brain tumors, Cancer Biology and Therapy 11 (2011) 974–980.
[36] P. Bernabei, E.M. Coccia, L. Rigamonti, M. Bosticardo, G. Forni, S. Pestka, C.D. Krause, A. Battistini, F. Novelli, Interferon-gamma receptor 2 expression as the deciding factor in human T, B, and myeloid cell proliferation or death, Journal of Leukocyte Biology 70 (2001) 950–960.
[37] H.W. Xin, D.M. Hari, J.E. Mullinax, C.M. Ambe, T. Koizumi, S. Ray, A.J. Anderson, G.W. Wiegand, S.H. Garfield, S.S. Thorgeirsson, I. Avital, Tumor-initiating label-retaining cancer cells in human gastrointestinal cancers undergo asymmetric cell division, Stem Cells 30 (2012) 591–598.
[38] P. Bragado, Y. Estrada, M.S. Sosa, A. Avivar-Valderas, D. Cannan, E. Genden, M. Teng, A.C. Ranganathan, H.C. Wen, A. Kapoor, E. Bernstein, J.A. Aguirre-Ghiso, Analysis of marker-defined HNSCC subpopulations reveals a dynamic regulation of tumor initiating properties, PloS One 7 (2012) e29974.
[39] Z. Xue, H. Yan, J. Li, S. Liang, X. Cai, X. Chen, Q. Wu, L. Gao, K. Wu, Y. Nie, D. Fan, Identification of cancer stem cells in vincristine preconditioned SGC7901 gastric cancer cell line, Journal of Cellular Biochemistry 113 (2012) 302–312.
[40] J.L. Dembinski, S. Krauss, Characterization and functional analysis of a slow cycling stem cell-like subpopulation in pancreas adenocarcinoma, Clinical and Experimental Metastasis 26 (2009) 611–623.
[41] A. Roesch, M. Fukunaga-Kalabis, E.C. Schmidt, S.E. Zabierowski, P.A. Brafford, A. Vultur, D. Basu, P. Gimotty, T. Vogt, M. Herlyn, A temporarily distinct subpopulation of slow-cycling melanoma cells is required for continuous tumor growth, Cell 141 (2010) 583–594.
[42] S. Pece, D. Tosoni, S. Confalonieri, G. Mazzarol, M. Vecchi, S. Ronzoni, L. Bernard, G. Viale, P.G. Pelicci, P.P. Di Fiore, Biological and molecular heterogeneity of breast cancers correlates with their cancer stem cell content, Cell 140 (2010) 62–73.
[43] T. Ishimoto, H. Oshima, M. Oshima, K. Kai, R. Torii, T. Masuko, H. Baba, H. Saya, O. Nagano, CD44+ slow-cycling tumor cell expansion is triggered by cooperative actions of Wnt and prostaglandin E2 in gastric tumorigenesis, Cancer Science 101 (2010) 673–678.
[44] L.P. Deleyrolle, A. Harding, K. Cato, F.A. Siebzehnrubl, M. Rahman, H. Azari, S. Olson, B. Gabrielli, G. Osborne, A. Vescovi, B.A. Reynolds, Evidence for label-retaining tumour-initiating cells in human glioblastoma, Brain: A Journal of Neurology 134 (2011) 1331–1343.
[45] R.K. Montgomery, D.L. Carlone, C.A. Richmond, L. Farilla, M.E. Kranendonk, D.E. Henderson, N.Y. Baffour-Awuah, D.M. Ambruzs, L.K. Fogli, S. Algra, D.T. Breault, Mouse telomerase reverse transcriptase (mTert) expression marks slowly cycling intestinal stem cells, Proceedings of the National Academy of Sciences of the United States of America 108 (2011) 179–184.
[46] E. Sangiorgi, M.R. Capecchi, Bmi1 is expressed in vivo in intestinal stem cells, Nature Genetics 40 (2008) 915–920.
[47] A.E. Powell, Y. Wang, Y. Li, E.J. Poulin, A.L. Means, M.K. Washington, J.N. Higginbotham, A. Juchheim, N. Prasad, S.E. Levy, Y. Guo, Y. Shyr, B.J. Aronow, K.M. Haigis, J.L. Franklin, R.J. Coffey, The pan-ErbB negative regulator Lrig1 is an intestinal stem cell marker that functions as a tumor suppressor, Cell 149 (2012) 146–158.
[48] K.S. Yan, L.A. Chia, X. Li, A. Ootani, J. Su, J.Y. Lee, N. Su, Y. Luo, S.C. Heilshorn, M.R. Amieva, E. Sangiorgi, M.R. Capecchi, C.J. Kuo, The intestinal stem cell markers Bmi1 and Lgr5 identify two functionally distinct populations, Proceedings of the National Academy of Sciences of the United States of America (2011).
[49] P.B. Gupta, C.M. Fillmore, G. Jiang, S.D. Shapira, K. Tao, C. Kuperwasser, E.S. Lander, Stochastic state transitions give rise to phenotypic equilibrium in populations of cancer cells, Cell 146 (2011) 633–644.
[50] A.G. Schepers, H.J. Snippert, D.E. Stange, M. van den Born, J.H. van Es, M. van de Wetering, H. Clevers, Lineage tracing reveals Lgr5+ stem cell activity in mouse intestinal adenomas, Science (2012).
[51] G. Driessens, B. Beck, A. Caauwe, B.D. Simons, C. Blanpain, Defining the mode of tumour growth by clonal analysis, Nature (2012).
[52] F. Novelli, P. Bernabei, L. Ozmen, L. Rigamonti, A. Allione, S. Pestka, G. Garotta, G. Forni, Switching on of the proliferation or apoptosis of activated human T lymphocytes by IFN-γ is correlated with the differential expression of the alpha- and beta-chains of its receptor, Journal of Immunology 157 (1996) 1935–1943.
[53] P. Bernabei, A. Allione, L. Rigamonti, M. Bosticardo, G. Losana, I. Borghi, G. Forni, F. Novelli, Regulation of interferon-gamma receptor (INF-γR) chains: a peculiar way to rule the life and death of human lymphocytes, European Cytokine Network 12 (2001) 6–14.
[54] G.H. Windbichler, H. Hausmaninger, W. Stummvoll, A.H. Graf, C. Kainz, J. Lahodny, U. Denison, E. Muller-Holzner, C. Marth, Interferon-gamma in the first-line therapy of ovarian cancer: a randomized phase III trial, British Journal of Cancer 82 (2000) 1138–1144.